

Transcriptomic and physiological responses of *Skeletonema costatum* to ATP utilization

Xiaohua Zhang^{1,2,3}, Senjie Lin⁴ and Dongyan Liu^{5*}

¹Key Laboratory of Coastal Zone Environmental Processes and Ecological Remediation, Yantai Institute of Coastal Zone Research, Chinese Academy of Sciences, Yantai, 264003, China.

²University of Chinese Academy of Sciences, Beijing, 100049, China.

³Department of Gene Engineering, Binzhou Medical University, Yantai, 264003, China.

⁴Department of Marine Sciences, University of Connecticut, Groton, CT, 06340, USA.

⁵State Key Laboratory of Estuarine and Coastal Research, East China Normal University, Shanghai, 200241, China.

Summary

The capacity of phytoplankton to utilize dissolved organic phosphorus (DOP) plays an important role in their competition for resources when the availability of dissolved inorganic phosphorus (DIP) is low in the aquatic systems. Here, we explored the physiological and molecular responses of a globally distributed marine diatom, *Skeletonema costatum*, in utilizing adenosine-5'-triphosphate (ATP) based on incubation experiments under ATP, DIP-replete, and DIP-depleted conditions. The results show that ATP supports the growth of *S. costatum* as efficiently as DIP. The pathway of *S. costatum* involved in utilizing ATP is not related to alkaline phosphatase (AP), an important DOP hydrolase, although extracellular hydrolysis is involved. The transcriptome analysis revealed several transcripts related to the hydrolase activity (e.g. NAD⁺ diphosphatase), which were significantly upregulated in the ATP culture group, indicating their possible involvement in ATP hydrolysis. Meanwhile, ATP-grown *S. costatum* exhibited downregulation of the genes related to a series of metabolic activities

(e.g. purine metabolism), apparently to adapt to ATP condition.

Introduction

Phosphorus (P) is an essential macronutrient for phytoplankton proliferation in the ocean, and its bioavailability to phytoplankton not only significantly influences the primary production but also the biogeochemical processes (Sanudo-Wilhelmy *et al.*, 2001; Dyhrman *et al.*, 2006; Hynes *et al.*, 2009). Bioavailable phosphorus in the ocean exists in two forms: dissolved inorganic phosphorus (DIP) and dissolved organic phosphorus (DOP) (Lin *et al.*, 2016). In general, phytoplankton prefer to uptake DIP, while some species are able to utilize DOP, particularly when the availability of DIP is limited (Ruttenberg and Dyhrman, 2005; Dyhrman and Ruttenberg, 2006; Mather *et al.*, 2008). Therefore, DOP is not only a major reservoir of phosphorus but also an important bioavailable resource that phytoplankton species compete for in DIP-deficient systems (Harke *et al.*, 2012).

The species capable of using DOP can not only better sustain their populations in interspecific competition but can also outgrow others to form harmful algal blooms. DOP has been regarded as one of the most important nutrient sources responsible for the large blooms of *Prorocentrum donghaiense* in the East China Sea (Ou *et al.*, 2019). Therefore, understanding DOP utilization efficiency and regulation mechanisms is an important research topic in phytoplankton ecology (Wang *et al.*, 2011; Li *et al.*, 2015; Diaz *et al.*, 2018). The hydrolysis of DOP is the most common and most acknowledged mechanisms to explain the pathway of DOP utilization (Reynolds *et al.*, 2014; Lin *et al.*, 2016). Alkaline phosphatase (AP) is advocated as the most important hydrolase that facilitates DOP utilization (Hoppe, 2003; Nicholson *et al.*, 2006).

It has been recognized that the physiological mechanism utilizing DOP in phytoplankton is complex. DOP exists in numerous chemical forms in the ocean and primarily contains phosphoesters (C–O–P-bonded compounds) and phosphonates (C–P-bonded compounds) (Lin *et al.*, 2016). Each compound has unique chemical properties, including susceptibility to phosphohydrolase. It

Received: 06 September 2019, revised: 13 February 2020
accepted: 14 February 2020. *For correspondence. E-mail
dylu@sklec.ecnu.edu.cn; Tel: (+86) 021 54836003; Fax:
(+86) 021 54836458.

is difficult to characterize individual compounds and only a few DOP compounds (e.g. ATP) have been measured in seawater (Karl and Björkman, 2015). Different species evolve different physiological pathways in DOP utilization. Besides AP, several other enzymes have been attributed to DOP hydrolysis, including 5'-nucleotidase (5NT) and phosphodiesterase (Dyhrman *et al.*, 2012; Yamaguchi *et al.*, 2014). The mechanisms and enzymes involved can vary between phytoplankton species and substrates. For instance, *Ditylum brightwellii* utilizes *sn*-glycero-3-phosphocholine via phosphodiesterase (Yamaguchi *et al.*, 2014) while *Chaetoceros ceratosporus* utilizes bis (*p*-nitrophenyl) phosphate by means of phosphodiesterase and alkaline phosphatase (Yamaguchi *et al.*, 2005). In the dinoflagellate *Karenia mikimotoi*, ATP utilization is implemented first by extracellular hydrolysis apparently via 5NT, but then also uptake of ADP/AMP, the products of ATP hydrolysis, via a novel transporter MOAT (Luo *et al.*, 2017). Contrastingly, in the same species, glucose-6-P is utilized by direct uptake (Zhang *et al.*, 2017). However, the molecular mechanism driving the physiological responses to diversify DOP utilization in phytoplankton remains poorly understood. Here, we chose diatom *Skeletonema costatum* as a model for the most abundant group of coastal phytoplankton to explore its physiological and molecular mechanisms in utilizing adenosine-5'-triphosphate (ATP), one of the ubiquitous forms of DOP in the ocean (Azam and Hodson, 1977; Hodson *et al.*, 1981).

Skeletonema costatum is a marine phytoplankton species that is distributed worldwide and often forms blooms in coastal waters (Boller *et al.*, 2015). Under the conditions of phosphorus limitation or starvation, this species utilizes DOP with the action of DOP hydrolases, e.g. AP, phospholipase A1, and phosphodiesterase (Moller *et al.*, 1975; Yamaguchi *et al.*, 2004; Zhang *et al.*, 2016). Thus, we designed the incubation experiments under ATP, DIP-replete, and DIP-depleted conditions to induce the activity of DOP hydrolase and examine the possible enzymes involved in DOP hydrolysis. Meanwhile, RNA-sequencing was conducted to compare the patterns of differential gene expression in *S. costatum* under ATP and DIP-replete conditions, in order to understand the molecular mechanisms of ATP utilization in *S. costatum*.

Results

Physiological responses of S. costatum under different phosphorus treatments

The growth curves of *S. costatum* under different phosphorus treatments diverged on day 3 (Fig. 1A). The cell density in the DIP-replete and ATP groups increased with a similar trend, reaching the peak on day 4 (7.3×10^5 cells mL⁻¹) and day 5 (7.8×10^5 cells mL⁻¹) respectively. In

contrast, the growth in the DIP-depleted group was depressed (Fig. 1A). The DOP concentration was barely detectable in the DIP-replete and DIP-depleted groups, while it decreased significantly in the ATP group within the first 5 days (Fig. 1B). These results indicated that ATP was consumed quickly and also supported the growth of *S. costatum* as efficiently as DIP. DIP concentration in the DIP-replete group decreased, but it increased in the ATP group within the first 5 days (Fig. 1C), indicating that there was a DIP release in the ATP group.

Interestingly, bulk APA was barely detectable in the ATP and DIP-replete groups during the experiment, both as measured for the collected cells and for the culture medium after the cells were removed. In contrast, it increased markedly in the DIP-depleted group (Fig. 1D). Live cells were obtained and labelled with ELF[®] 97 to detect the APA in single cell. ELF fluorescence (EF) labelling showed the same result as bulk APA detection (Fig. 2). EF appeared only in DIP-depleted cells (Fig. 1D). These results indicated that AP was expressed in *S. costatum* cells under phosphorus stress condition, but it was not involved in ATP hydrolysis.

Transcriptome sequencing, assembly, and annotation

RNA-seq in the ATP and DIP-replete groups was conducted to characterize differentially expressed genes related to ATP utilization. Totally, 53 837 854 raw reads were generated and 52 923 104 clean reads (7.94 G clean bases) remained after removing the low-quality sequences and adaptor sequences (Table 1). The clean reads were *de novo* assembled into 46 697 unigenes with a mean length of 1490 bp. Of the unigenes obtained, 35 638 (76.31%) matched with the homologues in at least one database with known functions (Supporting Information Table S2).

Identification of differentially expressed genes

We used DESeq2 (Love *et al.*, 2014) to screen differentially expressed genes (DEGs: $\text{padj} < 0.05$ $\log_2\text{FoldChangel} > 1$) between ATP and DIP-replete groups. Totally, 603 DEGs were identified, including 136 upregulated and 467 downregulated genes (Fig. 3). A complete list of DEGs and fold changes are presented in Supporting Information File S1. For GO enrichment analysis, all DEGs were mapped to GO terms in the database (Supporting Information File S1).

GO enrichment analysis of DEGs indicated that significant enrichment (corrected *P*-value < 0.05) concentrated on light harvesting, purine nucleotide salvage, and AMP salvage (Fig. 4). Based on the KEGG database, DEGs were functionally categorized into 43 KEGG pathways (Supporting Information File S1). The KEGG

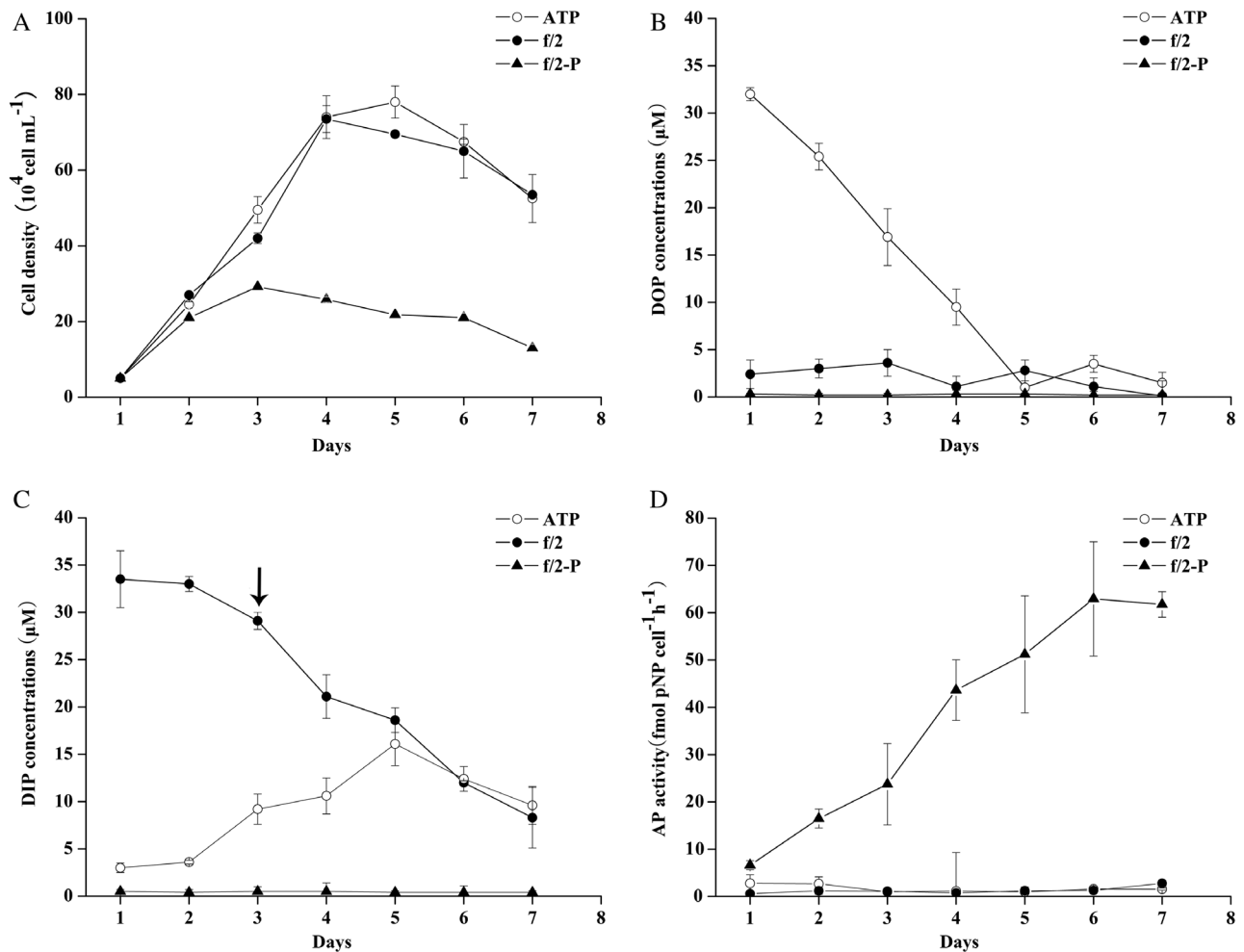


Fig. 1. Physiological characteristics of *Skeletonema costatum* under ATP, DIP-replete and DIP-depleted conditions. A. Growth curve of *S. costatum* under different P conditions. B. DOP concentration. C. DIP concentration in the culture media; the arrow indicates the time point of the harvest of samples for RNA extraction. D. AP activity of *S. costatum* cells. Bars indicate the standard deviations of mean data ($n = 3$).

enrichment analysis indicated that upregulated DEGs are enriched in nicotinate and nicotinamide metabolism as well as peroxisome and lysine biosynthesis. The downregulated DEGs are enriched in purine metabolism, photosynthesis-antenna proteins, and glycerolipid metabolism (P -value < 0.05) (Supporting Information Fig. S1). The variation in these pathways revealed a remodelling metabolism in *S. costatum* under ATP condition. The significant upregulated DEGs under ATP condition were investigated to identify key ATP utilization genes, however, AP and 5'-nucleotidase (5NT), the most likely enzymes related to DOP hydrolysis, were not found. It matches the results from the culture experiment (Figs. 1D and 2) and proves that AP is not involved in ATP hydrolysis.

Confirmation of transcriptome data by real-time quantitative PCR

To validate the gene expression profiles obtained from the RNA-Seq, we randomly selected six genes for real-time quantitative PCR analysis. Based on the RT-qPCR results, genes encoding silicate transporter (SiT), nitrate transporter (NRT), ribose-phosphate pyrophosphokinase (PRPS), and 1-acyl-sn-glycerol-3-phosphate acyltransferase (plsC) were downregulated under ATP condition (Fig. 5); NAD⁺ diphosphatase (NUDT12) and ATP-binding cassette sub-family B (ABCB1) were upregulated in the ATP group (Fig. 5). These RT-qPCR results were in agreement with the RNA-seq data, thereby confirming the quality and accuracy of the RNA-seq experiment.

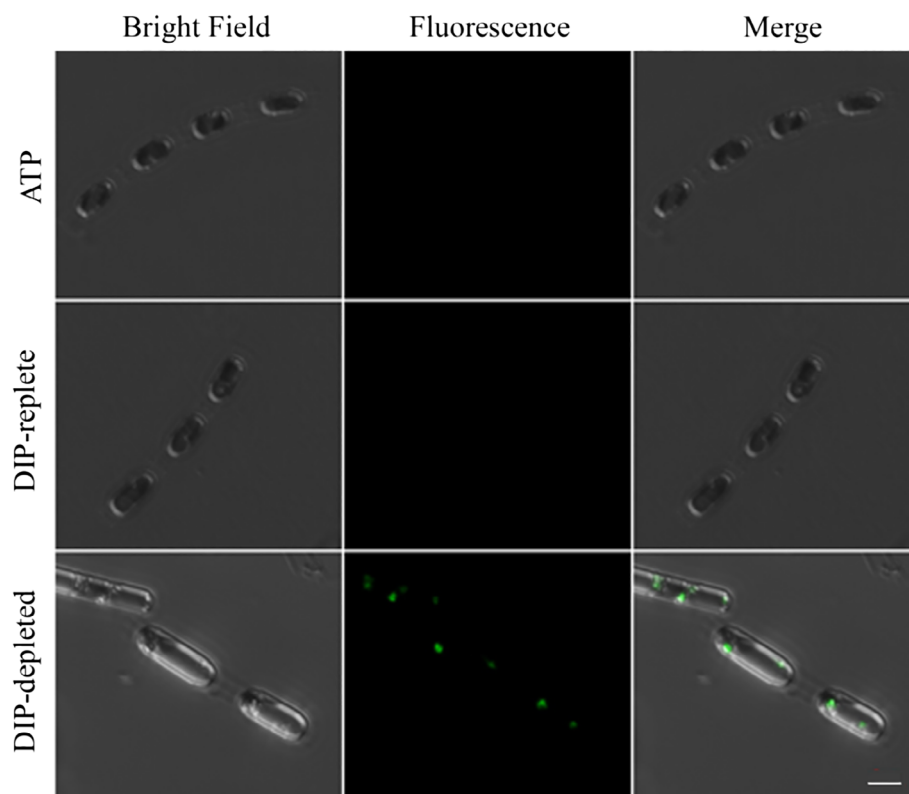


Fig. 2. Confocal microscopic images of ELF[®] 97 labelled *S. costatum* cells (with a $\times 3$ digital zoom). Scale bar = 5 μm . [Color figure can be viewed at wileyonlinelibrary.com]

Table 1. Summary of *Skeletonema costatum* transcriptome under ATP and DIP-replete conditions.

Sample	Raw reads	Clean reads	Clean bases	Error (%)	Q20 (%)	Q30 (%)	GC Content (%)
ATP 1	52 396 222	51 433 224	7.71G	0.02	97.98	94.43	47.8
ATP 2	53 837 854	52 923 104	7.94G	0.03	97.86	94.15	47.8
ATP 3	51 520 348	50 584 034	7.59G	0.02	97.97	94.48	47.93
DIP-replete 1	51 878 658	50 935 436	7.64G	0.03	97.83	94.1	47.96
DIP-replete 2	48 441 390	47 531 652	7.13G	0.02	97.99	94.41	47.8
DIP-replete3	51 874 662	50 740 440	7.61G	0.02	98.01	94.46	47.85

Discussion

ATP, one of the most important forms of DOP in the aquatic ecosystem and in the ocean, can be present in significant concentrations, e.g. >2.5 nM of peak concentrations, in the Southern Ocean (Azam and Hodson, 1977; Hodson *et al.*, 1981; Nawrocki and Karl, 1989). Phytoplankton such as dinoflagellates can take it up after hydrolysis (Krumhardt *et al.*, 2013; Luo *et al.*, 2017) or without hydrolysis (Li *et al.*, 2015). In this study, our detection of DIP release in the ATP medium clearly indicates that *S. costatum* hydrolyzes ATP before the uptake of the phosphorus (Fig. 1C). However, the enzyme activity (Fig. 1D) and gene analysis indicated that AP and 5NT, the most common enzymes for DOP hydrolysis (Dyhrman *et al.*, 2012; Lin *et al.*, 2016), are not involved in the ATP hydrolysis of *S. costatum*. The results reported here represent the first documentation of

physiological pathway and the distinct mechanism in any diatom, raising the need to further investigate the relationship between alkaline phosphatase and the utilization of other organic phosphorus (such as glucose-6-P) in *S. costatum*. This will further help uncover DOP utilization pathways in *S. costatum* and other diatoms.

In both plant and animal cells, extracellular ATP has been recognized as an important signalling molecule that induces diverse physiological responses (Torres *et al.*, 2008; Clark and Roux, 2009; Tanaka *et al.*, 2010). Transcriptomic analysis is an effective method to discover key corresponding genes and pathways for ATP utilization. Thus, we will discuss below the results from the transcriptomic analysis, in order to further explore the possible physiological and the molecular mechanisms of ATP utilization in *S. costatum* and metabolic processes influenced by the switch from DIP to ATP as a P-nutrient.

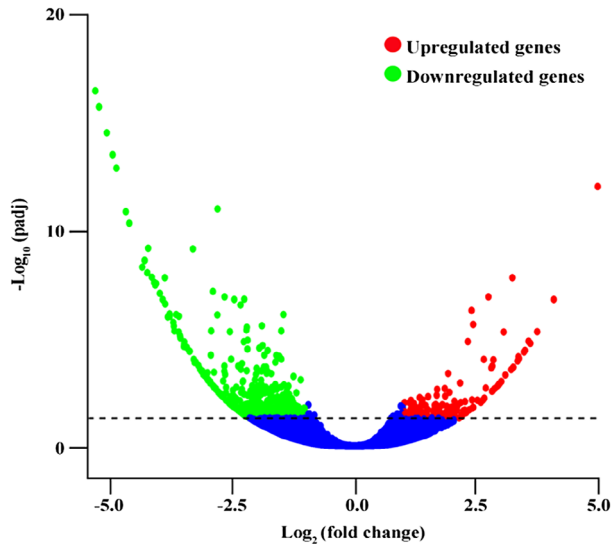


Fig. 3. Volcano map of differentially expressed genes (DEGs) in *S. costatum* between ATP and DIP-replete groups. $-\log_{10}$ adjusted p-values (padj) from the differential expression test were plotted against the \log_2 fold change for each informative gene. Each dot represents a gene (red dots: upregulated DEGs; green dots: downregulated DEGs; and blue dots: non-DEGs). [Color figure can be viewed at [wileyonlinelibrary.com](#)]

Upregulated genes

In this study, several transcripts related to the hydrolase activity showed upregulated levels in the ATP group (Supporting Information File S1). Among them, transcripts encoding NAD⁺ diphosphatase are particularly

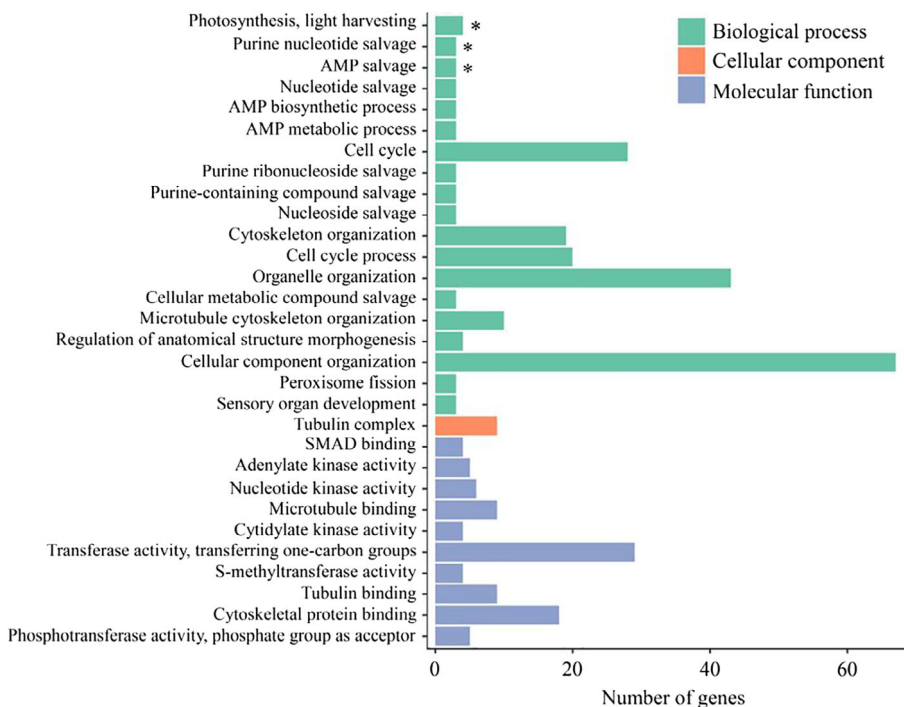


Fig. 4. GO analysis of differentially expressed genes (DEGs) between ATP and DIP-replete conditions. DEGs were classified into three functional categories: biological process, cellular component, and molecular function ($*P$ -value < 0.05). [Color figure can be viewed at [wileyonlinelibrary.com](#)]

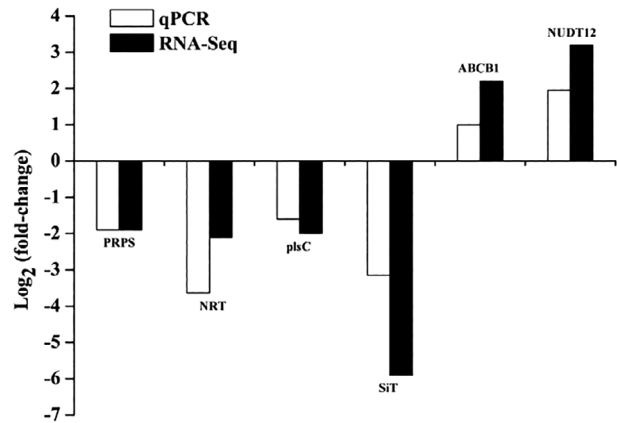


Fig. 5. RT-qPCR validations of differentially expressed genes. The relative expression level of each gene is presented as the ratio of the ATP and DIP-replete groups calculated as $\log_2(2^{-\Delta\Delta CT})$. β -Actin was used as an internal control for normalization. Gene name abbreviations: PRPS, ribose-phosphate pyrophosphokinase; NRT, nitrate transporter; plsC, 1-acyl-sn-glycerol-3-phosphate acyltransferase; SIT, silicate transporter; ABCB1, ATP-binding cassette subfamily B; NUDT12, NAD⁺ diphosphatase.

interesting, as this enzyme belongs to the subclass of Nudix hydrolases, which are found in all classes of organisms and hydrolyze a wide range of organic pyrophosphates, including nucleoside triphosphates (Nakajima *et al.*, 1973; Kraszewska, 2008). A transcript encoding nucleotide pyrophosphatase/phosphodiesterase is also found in the ATP group (Supporting Information File S1). It belongs to the ecto-nucleotide

pyrophosphatase/phosphodiesterase (E-NPP) family and hydrolyzes phosphates from nucleotide triphosphates (Zimmermann, 2000). In addition, a transcript encoding the P2X purinergic receptor was found to be significantly upregulated in the ATP group. The P2X purinergic receptor, which interacts with extracellular ATP to initiate signal transduction in animals (Clark and Roux, 2009), has also been identified in the green alga *Ostreococcus tauri* genome (Fountain *et al.*, 2008). This suggests that extracellular nucleotide signalling might exist in *S. costatum*, which could induce extracellular hydrolases as ectoapyrases to hydrolyze ATP, thereby providing DIP for cells and consuming ambient ATP.

Downregulated genes

Several genes involved in purine synthesis showed downregulated expression in the ATP group. Inosine monophosphate (IMP) is the first nucleotide formed during *de novo* purine biosynthesis. A key regulatory step is the production of 5-phospho- α -D-ribose 1-pyrophosphate (PRPP) by ribose phosphate pyrophosphokinase (PRPS1), which is activated by inorganic phosphate and inactivated by purine ribonucleotides (Hove-Jensen, 2004; Bibi *et al.*, 2016). The expression of PRPS1 is downregulated by more than 3.7-fold in the ATP group relative to the DIP-replete group. Phosphoribosylaminoimidazole carboxylase, known to catalyse the sixth step in the IMP biosynthesis in eukaryotes (Kanai and Toh, 1999), is also downregulated in the ATP group. Thus, the *de novo* pathway of purine nucleotides downregulated in the ATP group might have enriched the supply of purine in *S. costatum*. There is a possibility that some ATP hydrolysates are also transported into cells just as in the dinoflagellate *K. mikimotoi* (Luo *et al.*, 2017). In addition, transcripts of adenylate kinase (ADK) and adenine nucleotide translocator (ANT) were also downregulated in the ATP group. ADK catalyses the reversible transfer of the terminal phosphate group between ATP and AMP (Yang and Li, 2017) and is recognized as a sensitive reporter of the cellular energy state (Thieulin-Pardo *et al.*, 2016). ANT exchanges free ATP with free ADP across the inner mitochondrial membrane. These outcomes indicated decelerated nucleotide metabolism and reduction of ATP production in the ATP cultures.

Conclusions

Skeletonema costatum clearly exhibits a hydrolysis mechanism for ATP utilization in evolution; however, AP is not the enzyme that is responsible for ATP hydrolysis. The functions of transcripts encoding NAD⁺ diphosphatase and nucleotide pyrophosphatase/phosphodiesterase deserve to be further investigated for their potential roles

in ATP hydrolysis. Our transcriptomic analysis indicated an effect of ATP utilization on cell metabolism; *S. costatum* might regulate cellular metabolism to maintain their efficient growth under ATP condition.

Experimental procedures

Culture experiments

Skeletonema costatum was cultured in an incubator (Boxun, Shanghai, China) at 20°C and 55 $\mu\text{mol m}^{-2} \text{s}^{-1}$ in a 12/12 h light/dark cycle. Sterilized artificial seawater was prepared for the culture to simulate species growth in enriched natural seawater (Harrison *et al.*, 1980). The culture media used for the study included three groups, all based on f/2 medium: (i) DIP-replete group [f/2 medium that contained 36 μM DIP (NaH_2PO_4)], (ii) ATP group [f/2 medium with the replacement of DIP by 12 μM ATP (=36 μM P)] and (iii) DIP-depleted group (f/2 medium without added DIP). Each group was set up in triplicate. The culture media were inoculated with *S. costatum* cells at exponential growing phase with a starting concentration of 5×10^4 cells mL^{-1} . The samples were collected daily from each culture for analyses of cell concentration, DIP concentration in the medium, total dissolved P (TDP) concentration in the medium, and AP activity (APA) of the cells respectively.

The cell concentration was obtained using a 0.1 ml counting chamber (20 mm \times 20 mm) with three replicated counts for each sample. The samples for soluble phosphorus analysis were filtered through 0.45 μm PES, and soluble DIP was measured following the molybdenum blue method (Murphy and Riley, 1962). TDP was analysed according to the method of Jeffries *et al.* (1979) by using an acid (sulfuric acid) potassium persulfate ($\text{K}_2\text{S}_2\text{O}_8$) oxidation procedure. The difference between DIP and TDP was taken as DOP.

Bulk and single-cell APA assay

Bulk APA of the samples was measured daily as described previously (Lin *et al.*, 2012). Cell pellets of each group were collected daily by centrifugation at 4000g for 15 min (Eppendorf, Hamburg, Germany). The pellets were then lysed in 1 ml of Tris buffer. After centrifugation, 1 ml of the supernatant was mixed with 50 μl of 20 mM *p*-nitro-phenylphosphate (*p*-NPP prepared in 1 M pH 9.0 Tris buffer) in a sterile tube and incubated in the dark at 20°C for 2 h. A similar experiment was set up for the culture medium after the cells were collected. The sample was placed on ice to stop further enzymatic reaction and was centrifuged at 10 000g for 2 min. The supernatant was used for OD measurement at 405 nm on a Bio-Tek Epoch Microplate Spectrophotometer. Single-cell

APA was measured by labeling with ELF[®] 97 phosphatase substrate (Invitrogen, Carlsbad, CA, USA) at a final concentration of 0.25 mM (Gonzalez-Gil *et al.*, 1998). Each ELF sample was examined using a laser scanning confocal microscope (LSM 880; ZEISS, Jena, Germany) with a DAPI long-pass filter set.

RNA isolation and transcriptome sequencing

Cell pellets were collected by centrifugation at 4000 *g* at 20°C for 15 min on day 3 for each sample and stored at –80°C until further analysis. The rationale behind selecting the time point for transcriptomic analysis was that the DIP concentration in the ATP group began to show a significant increase on the third day, which likely corresponded to the time when significant changes occurred in the expression of ATP utilization related genes in *S. costatum*. Total RNA was separately extracted using the TRIzol method. The RNA quality was monitored using 1% agarose gels and NanoPhotometer[®] spectrophotometer (IMPLEN, CA, USA). The RNA concentration was measured using the Qubit[®] RNA Assay Kit in Qubit[®] 2.0 Fluorometer (Life Technologies, CA, USA). mRNA was purified from total RNA by using poly-T oligo-attached magnetic beads and then fragmented. The first-strand cDNA was synthesized using a random hexamer primer and M-MuLV Reverse Transcriptase. The second-strand cDNA synthesis was performed using DNA Polymerase I and RNase H. The standard Illumina protocol was thereafter followed to construct cDNA libraries of 250–300 bp in length. The libraries were sequenced on an Illumina HiSeq platform, and paired-end reads were generated. All reads have been submitted to the SRA database of GenBank (<https://www.ncbi.nlm.nih.gov/sra>) with the accession number PRJNA563119.

De novo assembly and sequencing data analysis

Clean reads were obtained by removing adapters, reads containing ploy-N, and low-quality reads from raw data. *De novo* assembly was carried out by using Trinity (Grabherr *et al.*, 2011) with min_kmer_cov set to 2, with all other parameters set to default. The longest transcript of each subcomponent was defined as ‘unigene’ for functional annotation. The function of the unigenes was annotated according to the following databases: the NCBI non-redundant protein sequences (Nr), the NCBI non-redundant nucleotide sequences (Nt), the Swiss-Prot protein database, the Protein family (Pfam), the Clusters of Orthologous Groups of Proteins (KOG/COG), the Kyoto Encyclopedia of Genes and Genomes (KEGG) Orthologue database (KO), and Gene Ontology (GO).

Gene expression analysis using RT-qPCR

The RNA used for sequencing was subjected to real-time quantitative PCR (RT-qPCR) to verify the RNA-Seq data regarding gene expression dynamics. According to the sequencing results, we randomly selected six genes for verification using RT-qPCR. The first-strand cDNA was synthesized from total RNA by using the first-strand cDNA synthesis kit (Quanshijin, Beijing, China) in a total volume of 20 µl, following the manufacturer’s instructions. All PCR reactions were performed on a LightCycler 96 (Roche) by using a SYBR Green PCR kit (Roche, Indianapolis, IN, USA). All reactions were analysed and conducted in triplicate. Beta-actin, a commonly used internal reference gene (Renault *et al.*, 2008; Alexander *et al.*, 2012), was chosen to normalize the expression of the target genes. Supporting Information Table S1 lists the specific primers of the six genes and the internal reference gene β-actin primers used in the study.

Acknowledgements

The authors appreciate the help of our colleague, Yujue Wang during sample analysis. The research was funded by the Natural Science Foundation of China (41876127, 41776116) and the Ministry of Science and Technology, China (2016YFE0133700 and 2016YFA0600904).

References

- Alexander, H., Jenkins, B.D., Ryneerson, T.A., Saito, M.A., Mercier, M.L., and Dyhrman, S.T. (2012) Identifying reference genes with stable expression from high throughput sequence data. *Front Microbiol* **3**: 385.
- Azam, F., and Hodson, R.E. (1977) Dissolved ATP in sea and its utilization by marine-bacteria. *Nature* **267**: 696–698.
- Bibi, T., Perveen, S., Aziz, I., Bashir, Q., Rashid, N., Imanaka, T., and Akhtar, M. (2016) Pcal_1127, a highly stable and efficient ribose-5-phosphate pyrophosphokinase from *Pyrobaculum caldifontis*. *Extremophiles* **20**: 821–830.
- Boller, A.J., Thomas, P.J., Cavanaugh, C.M., and Scott, K. M. (2015) Isotopic discrimination and kinetic parameters of RubisCO from the marine bloom-forming diatom, *Skeletonema costatum*. *Geobiology* **13**: 33–43.
- Clark, G., and Roux, S.J. (2009) Extracellular nucleotides: ancient signaling molecules. *Plant Sci* **177**: 239–244.
- Diaz, J.M., Holland, A., Sanders, J.G., Bulski, K., Mollett, D., Chou, C.W., *et al.* (2018) Dissolved organic phosphorus utilization by phytoplankton reveals preferential degradation of polyphosphates over phosphomonoesters. *Front Mar Sci* **5**: 380.
- Dyhrman, S.T., and Ruttenberg, K.C. (2006) Presence and regulation of alkaline phosphatase activity in eukaryotic phytoplankton from the coastal ocean: implications for dissolved organic phosphorus remineralization. *Limnol Oceanogr* **51**: 1381–1390.

- Dyhrman, S.T., Chappell, P.D., Haley, S.T., Moffett, J.W., Orchard, E.D., Waterbury, J.B., and Webb, E.A. (2006) Phosphonate utilization by the globally important marine diazotroph *Trichodesmium*. *Nature* **439**: 68–71.
- Dyhrman, S.T., Jenkins, B.D., Rynearson, T.A., Saito, M.A., Mercier, M.L., Alexander, H., *et al.* (2012) The transcriptome and proteome of the diatom *Thalassiosira pseudonana* reveal a diverse phosphorus stress response. *PLoS One* **7**: e33768.
- Fountain, S.J., Cao, L., Young, M.T., and North, R.A. (2008) Permeation properties of a P2X receptor in the green algae *Ostreococcus tauri*. *J Biol Chem* **283**: 15122–15126.
- Gonzalez-Gil, S., Keafer, B.A., Jovine, R.V.M., Aguilera, A., Lu, S.H., and Anderson, D.M. (1998) Detection and quantification of alkaline phosphatase in single cells of phosphorus-starved marine phytoplankton. *Mar Ecol Prog Ser* **164**: 21–35.
- Grabherr, M.G., Haas, B.J., Yassour, M., Levin, J.Z., Thompson, D.A., Amit, I., *et al.* (2011) Full-length transcriptome assembly from RNA-Seq data without a reference genome. *Nat Biotechnol* **29**: 644–652.
- Harke, M.J., Berry, D.L., Ammerman, J.W., and Gobler, C.J. (2012) Molecular response of the bloom-forming cyanobacterium, *Microcystis aeruginosa*, to phosphorus limitation. *Microb Ecol* **63**: 188–198.
- Harrison, P.J., Waters, R.E., and Taylor, F.J.R. (1980) A broad-spectrum artificial seawater medium for coastal and open ocean phytoplankton. *J Phycol* **16**: 28–35.
- Hodson, R.E., Maccubbin, A.E., and Pomeroy, L.R. (1981) Dissolved adenosine-triphosphate utilization by free-living and attached bacterioplankton. *Mar Biol* **64**: 43–51.
- Hoppe, H.G. (2003) Phosphatase activity in the sea. *Hydrobiologia* **493**: 187–200.
- Hove-Jensen, B. (2004) Heterooligomeric phosphoribosyl diphosphate synthase of *Saccharomyces cerevisiae* - combinatorial expression of the five PRS genes in *Escherichia coli*. *J Biol Chem* **279**: 40345–40350.
- Hynes, A.M., Chappell, P.D., Dyhrman, S.T., Doney, S.C., and Webb, E.A. (2009) Cross-basin comparison of phosphorus stress and nitrogen fixation in *Trichodesmium*. *Limnol Oceanogr* **54**: 1438–1448.
- Jeffries, D.S., Dieken, F.P., and Jones, D.E. (1979) Performance of the autoclave digestion method for total phosphorus analysis. *Water Res* **13**: 275–279.
- Kanai, S., and Toh, H. (1999) Identification of new members of the GS ADP-forming family from the de novo purine biosynthesis pathway. *J Mol Evol* **48**: 482–492.
- Karl, D.M., and Björkman, K.M. (2015) Dynamics of dissolved organic phosphorus. In *Biogeochemistry of Marine Dissolved Organic Matter*, Hansell, D.A., and Carlson, C. A. (eds), New York: Academic Press, pp. 233–334.
- Kraszewska, E. (2008) The plant Nudix hydrolase family. *Acta Biochim Pol* **55**: 663–671.
- Krumhardt, K.M., Callnan, K., Roache-Johnson, K., Swett, T., Robinson, D., Reistetter, E.N., *et al.* (2013) Effects of phosphorus starvation versus limitation on the marine cyanobacterium *Prochlorococcus* MED4 I: uptake physiology. *Environ Microbiol* **15**: 2114–2128.
- Li, M., Li, L., Shi, X., Lin, L., and Lin, S. (2015) Effects of phosphorus deficiency and adenosine 5'-triphosphate (ATP) on growth and cell cycle of the dinoflagellate *Prorocentrum donghaiense*. *Harmful Algae* **47**: 35–41.
- Lin, S., Litaker, R.W., and Sunda, W.G. (2016) Phosphorus physiological ecology and molecular mechanisms in marine phytoplankton. *J Phycol* **52**: 10–36.
- Lin, X., Zhang, H., Huang, B., and Lin, S. (2012) Alkaline phosphatase gene sequence characteristics and transcriptional regulation by phosphate limitation in *Karenia brevis* (Dinophyceae). *Harmful Algae* **17**: 14–24.
- Love, M.I., Huber, W., and Anders, S. (2014) Moderated estimation of fold change and dispersion for RNA-seq data with DESeq2. *Genome Biol* **15**: 550.
- Luo, H., Lin, X., Li, L., Lin, L., Zhang, C., and Lin, S. (2017) Transcriptomic and physiological analyses of the dinoflagellate *Karenia mikimotoi* reveal non-alkaline phosphatase-based molecular machinery of ATP utilisation. *Environ Microbiol* **19**: 4506–4518.
- Mather, R.L., Reynolds, S.E., Wolff, G.A., Williams, R.G., Torres-Valdes, S., Woodward, E.M.S., *et al.* (2008) Phosphorus cycling in the North and South Atlantic Ocean subtropical gyres. *Nat Geosci* **1**: 439–443.
- Moller, M., Mykkestad, S., and Haug, A. (1975) Alkaline and acid-phosphatases of marine diatoms *Chaetoceros affinis* var. *willei* (Gran) Hustedt and *Skeletonema costatum* (Grev) Cleve. *J Exp Mar Biol Ecol* **19**: 217–226.
- Murphy, J., and Riley, J.P. (1962) A modified single solution method for determination of phosphate in natural waters. *Anal Chim Acta* **26**: 31.
- Nakajima, Y., Fukunaga, N., Sasaki, S., and Usami, S. (1973) Purification and properties of NADP pyrophosphatase from *proteus vulgaris*. *Biochim Biophys Acta* **293**: 242–255.
- Nawrocki, M.P., and Karl, D.M. (1989) Dissolved ATP turnover in the Bransfield Strait, Antarctica during a spring bloom. *Mar Ecol Prog Ser* **57**: 35–44.
- Nicholson, D., Dyhrman, S., Chavez, F., and Paytan, A. (2006) Alkaline phosphatase activity in the phytoplankton communities of Monterey Bay and San Francisco Bay. *Limnol Oceanogr* **51**: 874–883.
- Ou, L., Qin, X., Shi, X., Feng, Q., Zhang, S., Lu, S., and Qi, Y. (2019) Alkaline phosphatase activities and regulation in three harmful *Prorocentrum* species from the coastal waters of the East China Sea. *Microb Ecol*. <https://doi.org/10.1007/s00248-019-01399-3>.
- Renault, S., Baudrimont, M., Mesmer-Dudons, N., Gonzalez, P., Mornet, S., and Brisson, A. (2008) Impacts of gold nanoparticle exposure on two freshwater species: a phytoplanktonic alga (*Scenedesmus subspicatus*) and a benthic bivalve (*Corbicula fluminea*). *Gold Bull* **41**: 116–126.
- Reynolds, S., Mahaffey, C., Roussenov, V., and Williams, R. G. (2014) Evidence for production and lateral transport of dissolved organic phosphorus in the eastern subtropical North Atlantic. *Global Biogeochem Cy* **28**: 805–824.
- Ruttenberg, K.C., and Dyhrman, S.T. (2005) Temporal and spatial variability of dissolved organic and inorganic phosphorus, and metrics of phosphorus bioavailability in an upwelling-dominated coastal system. *J Geophys Res-Oceans* **110**: C10S13. <https://doi.org/10.1029/2004JC002837>.
- Sanudo-Wilhelmy, S.A., Kustka, A.B., Gobler, C.J., Hutchins, D.A., Yang, M., Lwiza, K., *et al.* (2001)

- Phosphorus limitation of nitrogen fixation by *Trichodesmium* in the central Atlantic Ocean. *Nature* **411**: 66–69.
- Tanaka, K., Gilroy, S., Jones, A.M., and Stacey, G. (2010) Extracellular ATP signaling in plants. *Trends Cell Biol* **20**: 601–608.
- Thieulin-Pardo, G., Schramm, A., Lignon, S., Lebrun, R., Kojadinovic, M., and Gontero, B. (2016) The intriguing CP12-like tail of adenylate kinase 3 from *Chlamydomonas reinhardtii*. *FEBS J* **283**: 3389–3407.
- Torres, J., Rivera, A., Clark, G., and Roux, S.J. (2008) Participation of extracellular nucleotides in the wound response of *Dasycladus vermicularis* and *Acetabularia acetabulum* (Dasycladales, Chlorophyta). *J Phycol* **44**: 1504–1511.
- Wang, Z.H., Liang, Y., and Kang, W. (2011) Utilization of dissolved organic phosphorus by different groups of phytoplankton taxa. *Harmful Algae* **12**: 113–118.
- Yamaguchi, H., Arisaka, H., Otsuka, N., and Tomaru, Y. (2014) Utilization of phosphate diesters by phosphodiesterase-producing marine diatoms. *J Plankton Res* **36**: 281–285.
- Yamaguchi, H., Nishijima, T., Nishitani, H., Fukami, K., and Adachi, M. (2004) Organic phosphorus utilization and alkaline phosphatase production of 3 red tide phytoplankton. *Nippon Suisan Gakk* **70**: 123–130.
- Yamaguchi, H., Yamaguchi, M., Fukami, K., Adachi, M., and Nishijima, T. (2005) Utilization of phosphate diester by the marine diatom *Chaetoceros ceratosporus*. *J Plankton Res* **27**: 603–606.
- Yang, F., and Li, H. (2017) Expression of adenylate kinase fused MEK1R4F in *Escherichia coli* and its application in ERK phosphorylation. *Biotechnol Lett* **39**: 1553–1558.
- Zhang, C., Luo, H., Huang, L., and Lin, S. (2017) Molecular mechanism of glucose-6-phosphate utilization in the dinoflagellate *Karenia mikimotoi*. *Harmful Algae* **67**: 74–84.
- Zhang, S.F., Yuan, C.J., Chen, Y., Chen, X.H., Li, D.X., Liu, J.L., et al. (2016) Comparative transcriptomic analysis reveals novel insights into the adaptive response of *Skeletonema costatum* to changing ambient phosphorus. *Front Microbiol* **7**: 1476.
- Zimmermann, H. (2000) Extracellular metabolism of ATP and other nucleotides. *N-S Arch Pharmacol* **362**: 299–309.

Supporting Information

Additional Supporting Information may be found in the online version of this article at the publisher's web-site:

Figure S1 KEGG pathway enrichment of upregulated DEGs genes (A) and downregulated DEGs genes (B) between the ATP and DIP-replete conditions with the top 20 terms. 'Rich factor' represents the ratio of the number of DEGs in the pathway and the total number of genes that have been annotated in this pathway. The greater the rich factor, the greater the degree of enrichment.

Table S1: Primers used for RT-qPCR in this study

Table S2: Statistics of unigene annotation in public databases